Technical Note: D/GPS Modeling & Estimation

Paul F. Roysdon[†]

Abstract— **Many applications require high precision navigation whilst using low-cost consumer-grade inertial navigation systems. Common implementations use a single epoch Extended Kalman Filter (EKF) combined with a single frequency GPS receiver. However, if model errors or receiver noise are large, the measurement update to the EKF can be compromised. This article provides the background and notation for GPS, as well as Differential GPS (DGPS), and formulates a proposed method for estimating Ionospheric "truth". Real world experimental results are provided to demonstrate the DGPS performance, which eliminates the need for Ionospheric models, versus the GPS performance using the estimated Ionospheric "truth" model parameters.**

I. INTRODUCTION

A. GPS Background

The United States Global Positioning System (GPS) is the most widely applied Global Navigation Satellite System (GNSS), providing global Positioning-Velocity-Timing (PVT) services. Modern inexpensive GPS receivers with ceramic patch antennas typically achieve 3-8 meter positioning accuracy with the Standard Positioning Service (SPS) [1]. There are four GPS segments:

- Space Segment: the constellation of GPS satellites.
- Control Segment: run by the U.S. Air Force and responsible for the monitoring and operation of the Space Segment.
- User Segment: the user hardware and processing software for positioning, navigation, and timing.
- Ground Segment: the civilian tracking networks that provide the User Segment with reference stations, precise ephemerides, and real time services for differential GPS (DGPS).

The satellite constellation is designed to have at least four satellites in view at all times. Therefore there are 24 satellites distributed on 6 orbital (elliptical) planes, with a semi-major axis (largest radius) of $26,600 \ km$, inclination angle of 55° to the equator, and orbital period approximately $11 \ hr. \ 58 \ min.$. The signals from the GPS satellites are driven by an atomic clock (typically cesium which has the best long-term stability), with a fundamental frequency of $10.23 \ MHz$, from which two carrier signals are generated. The L1 channel (frequency = $1575.42 \ MHz$; wavelength = $19.0 \ cm$) multiplies the fundamental frequency by 154, while the L2 channel (frequency = $1227.60 \ MHz$; wavelength = $24.4 \ cm$) multiplies the frequency by 120. The second signal was designed for self-calibration of the signal delay due to the Earth's ionosphere.

[†]Ph.D. Candidate at the Department of Electrical Engineering, University of California, Riverside. proysdon@ece.ucr.edu.

There are three types of code on the carrier signals:
- The Coarse Acquisition (C/A) code.
- The Precise (P) code.
- The Navigation Message.

The C/A code, on the L1 channel, which repeats every $1 \ ms$, is a pseudo-random code generated by a known algorithm. The carrier can transmit the C/A code at $1.023 \ Mbps$ (million bits per second). The "chip length", or physical distance between binary transitions (between digits +1 and -1), is 293 metres. The C/A code contains the satellite clock time at which the signal was transmitted (with an ambiguity of $1 \ ms$).

The P code, identical on both the L1 and L2 channels, which repeats every 267 days, is transmitted at $10.23 \ Mbps$, with a chip length of 29.3 metres. Like the C/A code, the P code contains the satellite clock time at which the signal was transmitted, except with ten times the resolution. Unlike the C/A code, the P code is encrypted by a process known as "anti-spoofing".

The Navigation Message on the L1 channel, is transmitted at $50 \ bps$ on the L1 channel. It is a 1500 bit sequence, and therefore takes 30 seconds to transmit. The Navigation Message includes information on the Broadcast Ephemeris (satellite orbital parameters), satellite clock corrections, almanac data (a crude ephemeris for all satellites), ionosphere information, and satellite health status. Obtaining the Broadcast Ephemeris for the entire visible constellation takes 12 minutes. The Broadcast Ephemeris is updated every two hours by the Control Segment, and the Ephemeris message contains a sub-message indicating the time at which the Ephemeris parameters are valid.

B. DGPS Background

To achieve reliable higher precision positioning, DGPS may be employed, using either satellite-based corrections via the Wide Area Augmentation Service (WAAS) transmitted on the L1 channel by civilian geo-stationary satellites [2], or ground-based corrections via publicly available correction service, e.g. Continuously Operating Reference Station (CORS) [3], Nationwide Differential Global Positioning System (NDGPS) [4] and EUREF [5].

To facilitate the internet transport of the differential information, international standards e.g. RTCM [6] and NTRIP [7] were developed and published. As the mobile communication networks (4G LTE or WiFi) become readily available, the DGPS technique can be used in various scenarios.

The DGPS techniques aim to remove the spatial-common errors between the rover receiver and the base receiver. Standard DGPS requires that the global position of the base

station is well-surveyed such that the spatial-common errors can be calculated precisely. With a base station in the range of a few tens of kilometers, DGPS accuracy is on the order of $1m$ (1σ), growing at the rate of $1m$ per $150km$ of separation [8].

While, this article will focus on CORS DGPS via NTRIP, a robust systems should employ both WAAS and CORS data, in the event that the mobile communication data-link is unavailable.

II. GPS MEASUREMENT MODELS

GPS measurements are made through estimating the travel time of the electromagnetic signals broadcast from the satellite vehicle antenna to the rover antenna.

A. Pseudorange Observable

To calculate user position, the range to each satellite must be determined. However, due to atmospheric effects and clock errors, a pseudorange is modeled. The L1 and L2 pseudorange measurements for the i-th satellite at time t can be modeled as

$$\tilde{\rho}^i_{r_1}(t) = \|\mathbf{p}_r(t) - \mathbf{p}^i(t)\|_2 + c\delta t_r(t)$$
$$+ \frac{f_2}{f_1} I^i_r(t) + T^i_r(t) + M^i_{\rho_1}(t) + n^i_{\rho_1}(t), \quad (1)$$

$$\tilde{\rho}^i_{r_2}(t) = \|\mathbf{p}_r(t) - \mathbf{p}^i(t)\|_2 + c\delta t_r(t)$$
$$+ \frac{f_1}{f_2} I^i_r(t) + T^i_r(t) + M^i_{\rho_2}(t) + n^i_{\rho_2}(t), \quad (2)$$

where

- $\|\mathbf{p}_r - \mathbf{p}^i\|_2$ is the geometric distance between the rover position $\mathbf{p}_r \in \mathbb{R}^3$ and the i-th satellite vehicle position $\mathbf{p}^i \in \mathbb{R}^3$,
- $c = 2.99792458 \times 10^8$ m/s is the speed of light,
- $\delta t_r \in \mathbb{R}$ is the receiver clock bias which is identical to all channels of the receiver,
- $f_1 = 1575.42 MHz$ is the L1 carrier frequency,
- $f_2 = 1227.60 MHz$ is the L2 carrier frequency,
- I^i_r is the Ionospheric error due to dispersive atmospheric effects in the layer of the atmosphere with altitude between 50 and 1000 km,
- T^i_r is the Tropospheric error due to non-dispersive atmospheric effects in the lower part of the atmosphere extending from the surface to 50 km above the surface of the planet,
- $M^i_{\rho_1}$ and $M^i_{\rho_2}$ are the pseudorange multipath errors caused by signal reflections,
- $n^i_{\rho_1}$, $n^i_{\rho_2} \sim \mathcal{N}(0, \sigma^{i^2}_\rho)$ are the (non-common mode) pseudorange measurement noise.

In practice, the position of the satellite vehicle is estimated from the orbital data which is broadcast continuously, and updated every two hours, in a data format called Ephemeris. Updated orbital information, is valid for two hours, and is uplinked to each GPS satellite at $1783.74 MHz$ by the U.S. Air Force Control Center at Falcon Air Force Base, Colorado Springs, USA. Based on the Ephemeris data, the satellite orbit can be fit through the Kepler model [9]. Small fit errors

TABLE I
TABLE OF USER RANGE ERROR (URE) STANDARD DEVIATION AND TIME CORRELATION.

Common Mode Errors	L1, σ	Time correlation
Ionosphere	7-10 m	> 6 hr.
Troposphere	1 m	> 6 hr.
Sv Clock	2 m	2 hr.
Sv Ephemeris	2 m	2 hr.
Non-common Mode Errors		
Multipath	0.1-3.0 m	3-10 min.
Receiver Noise	0.1-0.7 m	< 1 min.

of each satellite orbit is unavoidable, and called ephemeris error E^i. The clock on the satellite is also estimated with error. Thus, the true range between the satellite vehicle and the rover can be represented as

$$\|\mathbf{p}_r - \mathbf{p}^i\|_2 = \|\mathbf{p}_r - \hat{\mathbf{p}}^i\|_2 + E^i + c\delta t^i, \quad (3)$$

where $\hat{\mathbf{p}}^i$ is the estimated satellite vehicle position from the ephemeris and δt^i is the residual satellite clock error after performing the correction by model coefficients contained in the Ephemeris message.

The various errors in eqn. (1) and (2) can be divided into two categories: common mode and non-common mode. The satellite related errors E^i and $c\delta t^i$ are common to all receivers using the same ephemeris. The atmospheric errors I^i_r and T^i_r are common to spatial nearby ($<$ 15-20km) receivers. The multipath errors $M^i_{\rho_j}$ and receiver noise $n^i_{\rho_j}$ depending on the local electromagnetic environment are non-common between different receivers. Rewriting the common mode error for the i-th satellite as

$$E^i_{cm1} \triangleq E^i + c\delta t^i + \frac{f_2}{f_1} I^i_r + T^i_r, \quad (4)$$

$$E^i_{cm2} \triangleq E^i + c\delta t^i + \frac{f_1}{f_2} I^i_r + T^i_r, \quad (5)$$

the eqn. (1) and (2) can be simplified as

$$\tilde{\rho}^i_{r_1}(t) = \|\mathbf{p}_r(t) - \hat{\mathbf{p}}^i(t)\|_2 + c\delta t_r(t) + E^i_{cm1}(t)$$
$$+ M^i_{\rho_1}(t) + n^i_{\rho_1}(t), \quad (6)$$

$$\tilde{\rho}^i_{r_2}(t) = \|\mathbf{p}_r(t) - \hat{\mathbf{p}}^i(t)\|_2 + c\delta t_r(t) + E^i_{cm2}(t)$$
$$+ M^i_{\rho_2}(t) + n^i_{\rho_2}(t). \quad (7)$$

Table II-A from [10] indicate the magnitude of the above errors and their respective time correlation.

B. Carrier Phase Observable

The GPS carrier phase, or *phase* is simply an *angle of rotation*, which is in units of *cycles*, and is directly related to the *frequency*, which is expressed in units of *cycles per second*.

The L1 and L2 carrier phase measurements $\tilde{\varphi}^i_{r1}$ and $\tilde{\varphi}^i_{r2}$ for the i-th satellite at time t can be modeled as

$$\lambda_1 \tilde{\varphi}_{r1}^i(t) = \|\mathbf{p}_r(t) - \hat{\mathbf{p}}^i(t)\|_2 + c\delta t_r(t) + \lambda_1 N_1^i(t)$$
$$+ E_{cm3}^i(t) + M_{\varphi_1}^i(t) + n_{\varphi_1}^i(t), \qquad (8)$$

$$\lambda_2 \tilde{\varphi}_{r2}^i(t) = \|\mathbf{p}_r(t) - \hat{\mathbf{p}}^i(t)\|_2 + c\delta t_r(t) + \lambda_2 N_2^i(t)$$
$$+ E_{cm4}^i(t) + M_{\varphi_2}^i(t) + n_{\varphi_2}^i(t), \qquad (9)$$

where

- λ_1 and λ_2 are the wavelength of the corresponding carrier signals,
- N^i is the ambiguous integers representing the unknown number of whole cycles,
- E_{cm3}^i and E_{cm4}^i are common mode errors similar to E_{cm1}^i and E_{cm2}^i detailed in Section II-A

$$E_{cm3}^i = E^i + c\delta t^i - \frac{f_2}{f_1} I_r^i + T_r^i, \qquad (10)$$

$$E_{cm4}^i = E^i + c\delta t^i - \frac{f_1}{f_2} I_r^i + T_r^i, \qquad (11)$$

- $M_{\varphi_1}^i$, $n_{\varphi_1}^i$, $M_{\varphi_2}^i$, $n_{\varphi_2}^i$ are non-common mode errors similar to those of pseudorange measurements.

Note that the magnitude of $M_{\varphi_1}^i, n_{\varphi_1}^i, M_{\varphi_2}^i, n_{\varphi_2}^i$ are typically less than 1% of the magnitude of the respective errors in pseudorange measurements [10]. When common mode errors can be mitigated, the carrier phase measurements allow position estimation at the centimeter level. While carrier phase measurements have much lower noise level, they are biased by the unknown (usually large) integer ambiguity $\{N^i\}$. This is because there is no direct measure of the total number phase cycles of the incoming GPS signal. If the GPS receiver looses count of the oscillations (because of signal obstruction or excessive noise), then a new integer parameter must be introduced to the model. This integer discontinuity in phase data is called *cycle-slip*.

One crucial fact: the integer value $N^i(t) \equiv N^i$ and is constant when the Phase-Lock-Loop (PLL) of the receiver for the corresponding channel of the i-th satellite is maintained (i.e., no cycle-slip). Thus, if N^i is estimated in previous epoch and no cycle-slip occurs, the estimated integer should be used for current and later epochs. In practice, the GPS receiver reports the lock status of the PLL.

The noise $\mathbf{n}_\varphi^i \sim \mathcal{N}(0, \sigma_\varphi^{i\,2})$ introduces centimeter $(10^{-2}m)$ level range errors.

C. Delta Pseudorange Observable

The Delta Pseudorange observable, often referred to as the Doppler observable, is actually a quantity of subsequent pseudorange measurements over a consecutive time interval.

The Doppler frequency can be expressed as

$$f_r = f_T \left(1 - \frac{\dot{R}}{c}\right) \qquad (12)$$

relates the frequency received by a user f_r to the rate of change of the range between the receiver and the transmitter, where f_T is the transmitted frequency, and $\dot{R}$ is the geometric range between the user and the transmitter. The Doppler shift is

$$f_r - f_T = f_T \frac{\dot{R}}{c}. \qquad (13)$$

In GPS receivers, the delta pseudorange is a measurement of the quantity

$$\Delta\rho(\tau_r(t)) = \rho_r^s(\tau_r(t)) - \rho_r^s(\tau_r(t) - T) \qquad (14)$$

where typically $T \leq 1.0$. This quantity is the change in range over the time interval $\tau_r \in [\tau_r(t) - T, \tau_r(t)]$:

$$\Delta\rho(\tau_r(t)) = \int_{\rho_r^s(\tau_r(t)-T)}^{\rho_r^s(\tau_r(t))} \dot{\rho}_r^s(q) dq. \qquad (15)$$

Therefore, if the delta pseudorange is divided by T it measures the average rate of change of the pseudorange over the indicate time interval. By the mean value theorem, there is a value of $q \in [\tau_r(t) - T, \tau_r(t))$ such that $\dot{\rho}_r^s(q) = \frac{1}{T}\Delta\rho(\tau_r(t))$. By this reasoning the delta pseudorange observable is often modeled as the rate of change of the pseudorange at the midpoint of the interval $\tau_r \in [\tau_r(t) - T, \tau_r(t)]$ and referred to as the Doppler observable.

Assuming that the receiver has and maintains phase lock over the interval $\tau_r \in [\tau_r(t) - T, \tau_r(t)]$ that is of interest, then the Doppler observable can be computed as

$$\Delta\rho(\tau_r(t)) = \lambda\left(\phi_r^i(\tau_r(t)) - \phi_r^i(\tau_r(t) - T)\right). \qquad (16)$$

It is reasonable to assume that the measurement of the Doppler shift (in Hz) at the receiver indicated time is

$$D(\tau_r(t)) = \frac{\Delta\rho(\tau_r(t))}{\lambda T}. \qquad (17)$$

The Doppler measurement model is

$$\lambda T D_r^s(\tau_r(t)) = (\rho_r^s(\tau_r(t)) - \rho_r^s(\tau_r(t) - T))$$
$$- c\Delta\dot{t}^i + \epsilon(\tau_r(t)). \qquad (18)$$

where the temporal differences for E^i, I_r^i, and T_r^i have been dropped because they are small relative to the other terms, $\epsilon(\tau_r(t))$ represents the measurement error due to multipath and receiver noise, and $\Delta\dot{t}^i = \Delta t^i(\tau_r) - \Delta t^i(\tau_r - T)$ is the (uncorrected) satellite clock drift rate. The symbol $\Delta\dot{t}^i$ is used instead of $\delta\dot{t}^i$ as a reminder to correct the Doppler measurement for the satellite clock drift rate.

Assuming that the line-of-sight vector from the satellite to the user, $\mathbf{h}^\mathsf{T}$, is available from the position solution, a linearized model for the Doppler measurement is

$$\lambda D_r^s = \mathbf{h}^\mathsf{T}(\mathbf{v}_r - \mathbf{v}^s) + c\Delta\dot{t}_r - c\Delta\dot{t}^i + \epsilon. \qquad (19)$$

where $\mathbf{v}_r$ is the velocity of the receiver, and $\mathbf{v}^s$ is the s-th satellite velocity. The satellite velocity computation is described in Section C.4 of [10]. The satellite clock drift rate $c\Delta\dot{t}^i$ is predicted by the broadcast model to be $a_{f1}T$, see Section C.1 of [10].

III. DGPS AND NETWORK TRANSPORT STANDARDS

This section reviews the differential GPS technique and the Internet transportation standard and framework for GNSS differential information transportation.

A. Differential GPS

In DGPS, it is assumed that there exists a nearby (within 15-20km) stationary (i.e., $\mathbf{p}_b(t) \equiv \mathbf{p}_b \in \mathbb{R}^3$) base station which can provide GPS measurements from the base station receiver to the rover. In other words, the following measurements are available to the rover,

$$
\begin{aligned}
\tilde{\rho}_{b_1}^i(t) = \|\mathbf{p}_b - \hat{\mathbf{p}}^i(t)\|_2 + c\delta t_b(t) \\
+ E_{cm1}^{ib}(t) + M_{\rho_1}^{ib}(t) + n_{\rho_1}^{ib}(t),
\end{aligned} \tag{20}
$$

$$
\begin{aligned}
\tilde{\rho}_{b_2}^i(t) = \|\mathbf{p}_b - \hat{\mathbf{p}}^i(t)\|_2 + c\delta t_b(t) \\
+ E_{cm2}^{ib}(t) + M_{\rho_2}^{ib}(t) + n_{\rho_2}^{ib}(t),
\end{aligned} \tag{21}
$$

$$
\begin{aligned}
\lambda_1 \tilde{\varphi}_{b1}^i(t) = \|\mathbf{p}_b - \hat{\mathbf{p}}^i(t)\|_2 + c\delta t_b(t) + \lambda N_1^{ib}(t) \\
+ E_{cm3}^{ib}(t) + M_{\varphi_1}^{ib}(t) + n_{\varphi_1}^{ib}(t),
\end{aligned} \tag{22}
$$

$$
\begin{aligned}
\lambda_2 \tilde{\varphi}_{b2}^i(t) = \|\mathbf{p}_b - \hat{\mathbf{p}}^i(t)\|_2 + c\delta t_b(t) + \lambda N_2^{ib}(t) \\
+ E_{cm4}^{ib}(t) + M_{\varphi_2}^{ib}(t) + n_{\varphi_2}^{ib}(t).
\end{aligned} \tag{23}
$$

Base stations should be established in a good electromagnetic environment (e.g. on the top of the hill or high building with open sky, no multipath effects), such that it is valid to assume that $M_{\rho_1}^{ib} = M_{\rho_2}^{ib} = M_{\varphi_1}^{ib} = M_{\varphi_2}^{ib} \equiv 0$. Furthermore, the base position $\mathbf{p}_b$ should be well surveyed with respect to the global frame, such that with the differential technique, more precise global positioning can be realized. Herein, with the known base station position $\mathbf{p}_b$, four corrections are defined for later convenience,

$$
\alpha_1^i(t) \triangleq \tilde{\rho}_{b_1}^i(t) - \|\mathbf{p}_b - \hat{\mathbf{p}}^i(t)\|_2, \tag{24}
$$

$$
\alpha_2^i(t) \triangleq \tilde{\rho}_{b_2}^i(t) - \|\mathbf{p}_b - \hat{\mathbf{p}}^i(t)\|_2, \tag{25}
$$

$$
\alpha_3^i(t) \triangleq \lambda_1 \tilde{\varphi}_{b1}^i(t) - \|\mathbf{p}_b - \hat{\mathbf{p}}^i(t)\|_2, \tag{26}
$$

$$
\alpha_4^i(t) \triangleq \lambda_2 \tilde{\varphi}_{b2}^i(t) - \|\mathbf{p}_b - \hat{\mathbf{p}}^i(t)\|_2. \tag{27}
$$

Assuming no multipath at the base station antenna, these four corrections can be modeled as

$$
\alpha_1^i(t) = E_{cm1}^{ib}(t) + c\delta t_b(t) + n_{\rho_1}^{ib}(t), \tag{28}
$$

$$
\alpha_2^i(t) = E_{cm2}^{ib}(t) + c\delta t_b(t) + n_{\rho_2}^{ib}(t), \tag{29}
$$

$$
\alpha_3^i(t) = E_{cm3}^{ib}(t) + c\delta t_b(t) + \lambda N_1^{ib}(t) + n_{\varphi_1}^{ib}(t), \tag{30}
$$

$$
\alpha_4^i(t) = E_{cm4}^{ib}(t) + c\delta t_b(t) + \lambda N_2^{ib}(t) + n_{\varphi_2}^{ib}(t). \tag{31}
$$

If the base station is close to the rover, the following identity is valid

$$
E_{cm1}^i(t) = E_{cm1}^{ib}(t), \tag{32}
$$

$$
E_{cm2}^i(t) = E_{cm2}^{ib}(t), \tag{33}
$$

$$
E_{cm3}^i(t) = E_{cm3}^{ib}(t), \tag{34}
$$

$$
E_{cm4}^i(t) = E_{cm4}^{ib}(t). \tag{35}
$$

Since the satellite related errors E^i and $c\delta t^i$ are common to all receivers at the same epoch, only the atmospheric errors I_r^i and T_r^i depend on the locations. If $\{\alpha_j^i(t)\}_{j=1}^4$ is well known, then the raw rover measurements at the same epoch

t can be compensated as,

$$
{}^{\alpha}\tilde{\rho}_{r_1}^{id} = \tilde{\rho}_{r_1}^i - \alpha_1^i, \tag{36}
$$

$$
{}^{\alpha}\tilde{\rho}_{r_2}^{id} = \tilde{\rho}_{r_2}^i - \alpha_2^i, \tag{37}
$$

$$
\lambda_1 {}^{\alpha}\tilde{\varphi}_{r1}^{id} = \lambda_1 \tilde{\varphi}_{r1}^i - \alpha_3^i, \tag{38}
$$

$$
\lambda_2 {}^{\alpha}\tilde{\varphi}_{r2}^{id} = \lambda_2 \tilde{\varphi}_{r2}^i - \alpha_4^i \tag{39}
$$

The measurements defined in eqns. (36)-(39) are often referred as the *single-differenced* measurements with the model

$$
\begin{aligned}
{}^{\alpha}\tilde{\rho}_{r_1}^{id}(t) = \|\mathbf{p}_r(t) - \hat{\mathbf{p}}^i(t)\|_2 + c\delta t_{rb}(t) \\
+ M_{\rho_1}^i(t) + n_{\rho_1}^{id}(t),
\end{aligned} \tag{40}
$$

$$
\begin{aligned}
{}^{\alpha}\tilde{\rho}_{r_2}^{id}(t) = \|\mathbf{p}_r(t) - \hat{\mathbf{p}}^i(t)\|_2 + c\delta t_{rb}(t) \\
+ M_{\rho_2}^i(t) + n_{\rho_2}^{id}(t),
\end{aligned} \tag{41}
$$

$$
\begin{aligned}
\lambda_1 {}^{\alpha}\tilde{\varphi}_{r1}^{id}(t) = \|\mathbf{p}_r(t) - \hat{\mathbf{p}}^i(t)\|_2 + c\delta t_{rb}(t) \\
+ \lambda_1 N_1^{id}(t) + M_{\varphi_1}^i(t) + n_{\varphi_1}^{id}(t),
\end{aligned} \tag{42}
$$

$$
\begin{aligned}
\lambda_2 {}^{\alpha}\tilde{\varphi}_{r2}^{id}(t) = \|\mathbf{p}_r(t) - \hat{\mathbf{p}}^i(t)\|_2 + c\delta t_{rb}(t) \\
+ \lambda_2 N_2^{id}(t) + M_{\varphi_2}^i(t) + n_{\varphi_2}^{id}(t),
\end{aligned} \tag{43}
$$

where $\delta t_{rb} \triangleq \delta t_r - \delta t_b \in \mathbb{R}$ and $N_j^{id} \triangleq N_j^i - N_j^{ib} \in \mathbb{N}, j = 1, 2$ are the differenced clock bias and the differenced integer between the rover receiver and the base receiver, as well as the noise

$$
n_{\rho_1}^{id} \triangleq n_{\rho_1}^i - n_{\rho_1}^{ib}, \tag{44}
$$

$$
n_{\rho_2}^{id} \triangleq n_{\rho_2}^i - n_{\rho_2}^{ib}, \tag{45}
$$

$$
n_{\varphi_1}^{id} \triangleq n_{\varphi_1}^i - n_{\varphi_1}^{ib}, \tag{46}
$$

$$
n_{\varphi_2}^{id} \triangleq n_{\varphi_2}^i - n_{\varphi_2}^{ib}. \tag{47}
$$

In DGPS applications, the single-differenced measurements are used for positioning, instead of using the raw measurements in eqns. (1), (2), (8), (9). DGPS provides higher accuracy since the common mode errors are compensated. Since the common mode errors are time-varying, the rover measurements should be compensated with the base correction at the same epoch. In post-processing, the time-stamp correspondence can be realized by matching the GPS time-of-week of the measurements. However, in real-time implementations, the differential data transportation from the base station is delayed. Time correlation and delay of corrections is discussed in a later section.

B. DGPS Single Differencing

The single difference is used to remove satellite clock bias and atmospheric errors. The single difference geometry can be simplified as shown in Fig. 1, where the observations, L, for two receivers, A and B, observing the same satellite, j:

$$
L_A^j = \rho_A^j - \|\mathbf{p}_A - \hat{\mathbf{p}}^j\| + c\delta_A + c\delta^j + T_A^j - I_A^j + M_A^j + n_A^j
$$

$$
L_B^j = \rho_B^j - \|\mathbf{p}_B - \hat{\mathbf{p}}^j\| + c\delta_B + c\delta^j + T_B^j - I_B^j + M_B^j + n_B^j.
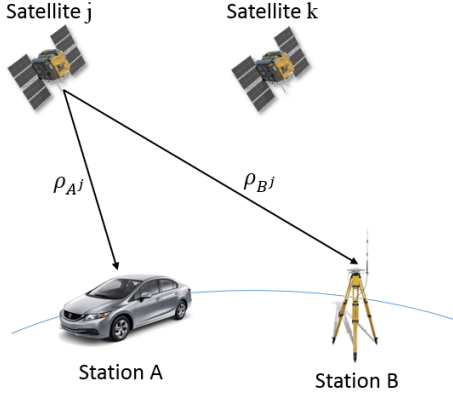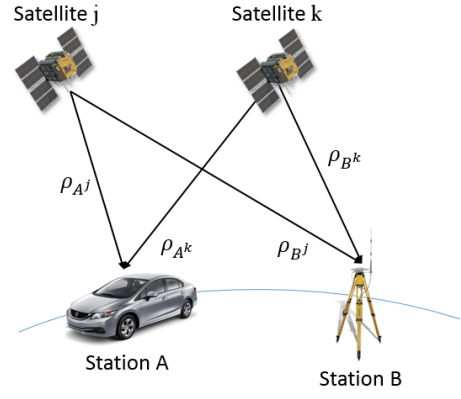$$

Fig. 1. Single differencing geometry.

Fig. 2. Double differencing geometry.

The single difference phase is defined as

$$
\begin{aligned}
\Delta L_{AB}^j &\equiv L_A^j - L_B^j \\
&= (\rho_A^j + c\delta_A + c\delta^j + T_A^j - I_A^j + M_A^j) \\
&\quad - (\rho_B^j + c\delta_B + c\delta^j + T_B^j - I_B^j + M_B^j) \\
&= (\rho_A^j - \rho_B^j) + (c\delta_A - c\delta_B) - (c\delta^j - c\delta^j) \\
&\quad + (T_A^j - T_B^j) - (I_A^j - I_B^j) + (M_A^j - M_B^j) \\
&= \Delta\rho_{AB}^j + c\Delta\delta_{AB} + \Delta T_{AB}^j - \Delta I_{AB}^j + \Delta M_{AB}^j.
\end{aligned}
$$

The double-subscript denotes the quantities identified with two receivers, and the Δ symbol is a mnemonic device to emphasize that the difference is made between two points on the ground. The above equations make the assumption that the satellite clock bias, δ^j, is identical for both receivers. While the difference in transmission time of the satellite to each base station could be as much as a few milli-seconds: over a milli-second (10^{-3} sec.) the satellite clock error will differ by 10^{-12} sec., which translates to a distance error of $10^{-12}c$, or $0.3\ mm$, which is negligible under most conditions.

The atmospheric delay terms are now considerably reduce, and vanish in the limit that the receivers are standing side-by-side. Differential troposphere can usually be ignored for horizontal separations less than $30\ km$, however the differences in height should be modeled. Differential ionosphere can usually be ignored for separations less than $30\ km$, depending on ionospheric conditions, however it is recommended to calibrate the ionospheric uncertainty using a dual-frequency receiver for separation distances larger than a few kilometers.

While the single difference method reduces or eliminates many of the error sources, only a relative position can be calculated. Furthermore, the receiver clock bias is still unknown.

C. DGPS Double Differencing

The double difference is used to remove receiver clock bias. The double difference geometry can be simplified as shown in Fig. 2, where the single difference observations for two receivers, A and B, observing satellites, j and k,

such that

$$
\begin{aligned}
\Delta L_{AB}^j &= \Delta\rho_{AB}^j + c\Delta\delta_{AB} + \Delta T_{AB}^j - \Delta I_{AB}^j + \Delta M_{AB}^j \\
\Delta L_{AB}^k &= \Delta\rho_{AB}^k + c\Delta\delta_{AB} + \Delta T_{AB}^k - \Delta I_{AB}^k + \Delta M_{AB}^k
\end{aligned}
$$

The double difference phase is defined as

$$
\nabla\Delta L_{AB}^{jk} \equiv \Delta L_{AB}^j - \Delta L_{AB}^k \tag{48}
$$

$$
\begin{aligned}
&= (\Delta\rho_{AB}^j + c\Delta\delta_{AB} + \Delta T_{AB}^j - \Delta I_{AB}^j + \Delta B_{AB}^j) \\
&\quad - (\Delta\rho_{AB}^k + c\Delta\delta_{AB} + \Delta T_{AB}^k - \Delta I_{AB}^k + \Delta B_{AB}^k)
\end{aligned} \tag{49}
$$

$$
\begin{aligned}
&= (\Delta\rho_{AB}^j - \Delta\rho_{AB}^k) + (c\Delta\delta_{AB} - c\Delta\delta_{AB}) \\
&\quad + (\Delta T_{AB}^j - \Delta T_{AB}^k) - (\Delta I_{AB}^j - \Delta I_{AB}^k) \\
&\quad + (\Delta B_{AB}^j - \Delta B_{AB}^k)
\end{aligned} \tag{50}
$$

$$
= \nabla\Delta\rho_{AB}^{jk} + \nabla\Delta T_{AB}^{jk} - \nabla\Delta I_{AB}^{jk} + \nabla\Delta B_{AB}^{jk} \tag{51}
$$

The double-superscript denotes the quantities identified with two satellites, and the symbol ∇ is a mnemonic device to emphasize that the difference is made between two points in the sky.

Note: while the receiver clock error is eliminated to the first-order, the residual effect due to *time tag bias* on the computation of the range term does not completely cancel. Also, any systematic effects due to unmodeled atmospheric errors are generally increased slightly by double differencing. Similarly, random errors due to noise or multipath are also increased.

Finally, double differencing reduces the phase ambiguity to an integer value, such that

$$
\nabla\Delta B_{AB}^{jk} \equiv \Delta B_{AB}^j - \Delta B_{AB}^k \tag{52}
$$

$$
= (\Delta B_A^j - \Delta B_B^j) - (\Delta B_A^k - \Delta B_B^k) \tag{53}
$$

$$
\begin{aligned}
&= \lambda_0(\psi_{0A} - \psi_0^j - N_A^j) - \lambda_0(\psi_{0B} - \psi_0^j - N_B^j) \\
&\quad - \lambda_0(\psi_{0A} - \psi_0^j - N_A^j) - \lambda_0(\psi_{0B} - \psi_0^j - N_B^j)
\end{aligned} \tag{54}
$$

$$
= -\lambda_0(N_A^j - N_B^j - N_A^k + N_B^k) \tag{55}
$$

$$
= -\lambda_0\nabla\Delta N_{AB}^{jk}. \tag{56}
$$

The double differenced phase observation equation is

$$\nabla\Delta L_{AB}^{jk} = \nabla\Delta\rho_{AB}^{jk} + \nabla\Delta T_{AB}^{jk} - \nabla\Delta I_{AB}^{jk} - \lambda_0\nabla\Delta N_{AB}^{jk}. \tag{57}$$

While the sign of $\lambda_0\nabla\Delta N_{AB}^{jk}$ is not important, the partial derivative must have a consistent sign.

D. DGPS Triple Differencing

The triple difference is used to remove the integer ambiguity. The triple difference geometry can be simplified as shown in Fig. 3, where the double difference observations
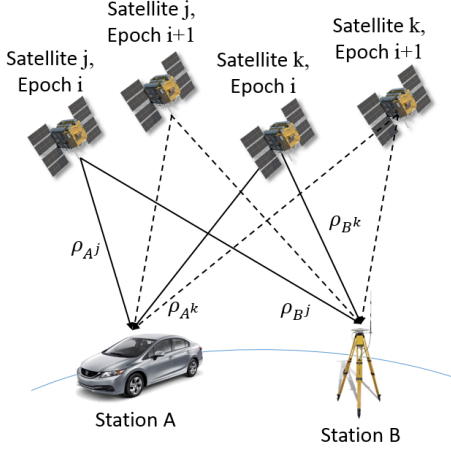
Fig. 3. Triple differencing geometry.

for two receivers, A and B, observing satellites, j and k, over two successive epochs $(i, i+1)$, such that

$$\nabla\Delta L_{AB}^{jk}(i) = \nabla\Delta\rho_{AB}^{jk}(i) + \nabla\Delta T_{AB}^{jk}(i)$$
$$- \nabla\Delta I_{AB}^{jk}(i) - \lambda_0\nabla\Delta N_{AB}^{jk} \tag{58}$$
$$\nabla\Delta L_{AB}^{jk}(i+1) = \nabla\Delta\rho_{AB}^{jk}(i+1) + \nabla\Delta T_{AB}^{jk}(i+1)$$
$$- \nabla\Delta I_{AB}^{jk}(i+1) - \lambda_0\nabla\Delta N_{AB}^{jk} \tag{59}$$
$$\tag{60}$$

The triple difference phase is defined as

$$\delta(i, i+1)\nabla\Delta L_{AB}^{jk} \equiv \nabla\Delta L_{AB}^{jk}(i) - \nabla\Delta L_{AB}^{jk}(i+1) \tag{61}$$
$$= \delta(i, i+1)\nabla\Delta\rho_{AB}^{jk}$$
$$+ \delta(i, i+1)\nabla\Delta T_{AB}^{jk}$$
$$- \delta(i, i+1)\nabla\Delta I_{AB}^{jk} \tag{62}$$
$$\tag{63}$$

The $\delta(i, i+1)$ denotes the quantities identified two epochs.

The triple difference only removes the integer ambiguity if it has not changed during the time interval between epochs. Any cycle-slips will appear as outliers. While triple differencing introduces time correlations between observations, it is useful for determining the ambiguous integer for double difference processing.

Efficient methods for solving the integer ambiguity are presented in [11], [12], and [13].

E. RTCM and NTRIP Standards

To transmit the differential GNSS message, non-proprietary and efficient protocols are highly desired. For this purpose, the Special Committee 104 on DGNSS of the Radio Technical Commission for Maritime Services (RTCM) proposed a standard for the dissemination of the differential information in binary messages [6]. This standard is usually referred as the RTCM standard, and the current version is 3.2.

"Networked Transport of RTCM via Internet Protocol" (NTRIP) stands for an application-level protocol on the Transmission Control Protocol/Internet Protocol (TCP/IP) stack, streaming GNSS data over the Internet. NTRIP is a generic, stateless protocol based on the Hypertext Transfer Protocol (HTTP/1.1) and the Real Time Streaming Protocol (RTSP). NTRIP is designed for disseminating differential correction data (e.g. in RTCM format) or other kinds of GNSS streaming data, to stationary or mobile users, over the Internet.

NTRIP consists of three system software components: clients, servers and casters. Fig. 4 shows the basic structure of a NTRIP system. In a typical NTRIP system, NTRIP servers transmit the RTCM message generated from base station receivers to the NTRIP Caster. One NTRIP Caster can carry multiple NTRIP servers. NTRIP Clients on the rover would request single or multiple NTRIP streams from NTRIP Caster with valid authorizations. By parsing the RTCM message in the NTRIP stream, the differential information (e.g. base receiver measurements or corrections) can be obtained. Fig. 5 shows the basic structure of the DGPS positioning routine on the rover: NTRIP client communicates with the NTRIP caster to get the required RTCM stream, then the binary RTCM messages are unpacked into engineering units by a parser, then the differential correction is calculated (see Section III-A). After compensating the rover measurements with differential corrections, DGPS positioning can be executed.
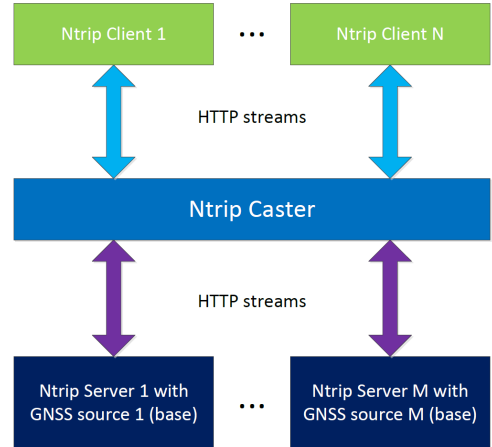

Fig. 4. Ntrip system structure with Ntrip Casters, Ntrip Servers, Ntrip Clients and base stations.
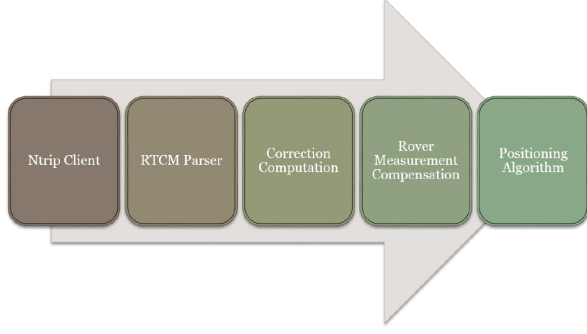
Fig. 5. Structure of the positioning routine of the rover with a Ntrip client.

IV. REAL-TIME ROBUST CORRECTION CALCULATION

As shown in Section III, the key procedure in DGPS is to compute the correction $\{\alpha_j^i(t)\}_{j=1}^4$. While internet is widely available, due to the development of network technology and infrastructures, transport delays of the differential data is still possible due to various reasons, e.g. limited 4G or LTE signal coverage. Thus, the base corrections cannot be calculated in real-time. Furthermore, if the differential data is from a temporary base station equipped with a low cost antenna and receiver, or immersed in a noisy electromagnetic environment, there may exist outliers in the base measurements. This section presents a base correction calculation method which can improve the real-time performance of DGPS and ensure robustness of the correction calculation.

Without loss of generality, let us only consider the correction calculation of L1 code and phase measurements. The proposed method can be easily extended to dual frequency cases. The description of the correction calculation problem can be stated as follows: given that

- the surveyed base ECEF (Earth-Centered-Earth-Fixed) position $\mathbf{p}_b \in \mathbb{R}^3$,
- circular buffers for each satellite maintain the code and phase measurements $\{\tilde{\rho}_{b_1}^i(t_{k-d})\}, k = 1, \ldots, K$ and $\{\lambda_1 \tilde{\varphi}_{b1}^i(t_{k-d})\}, k = 1, \ldots, K$, where $d \in \mathbb{N}$ indicates the natural number delay in epoch numbers and K is the circular buffer length,
- the satellite vehicle ECEF positions $\{\hat{\mathbf{p}}^i(t_{k-d})\}$ estimated with the ephemeris from the rover receiver,

the real-time corrections $\{\alpha_j^i(t_K)\}_{j=1}^4$ defined in eqns. (24)-(27) are expected to be estimated, where t_K indicates the time-of-week of the latest GPS measurement from the rover receiver.

The above problem statement implies that the real-time differential correction calculation with delayed data is a regression/prediction problem. To decide the proper model for this regression, the patterns of the corrections $\{\alpha_j^i(t_K)\}_{j=1}^4$ are first investigated. In Fig. 6, the differential corrections $\alpha_1^i(t)$ for L1 code measurements of different satellites are plotted with different color over a $1000s$ time interval. Two instant observations can be derived from Fig. 6:

- $\alpha_1^i(t)$ has a high frequency (fast-varying) and a low frequency (slowly-varying) components;

- the high frequency components for different satellites have similar pattern.

Since the satellite related errors E^i and $c\delta t^i$ and the atmospheric errors I_r^i and T_r^i are all slowly-varying signals, the common mode errors defined in eqns. (4)-(11) are the low frequency components in $\alpha_1^i(t)$. On the other hand, Fig. 7 shows the estimated GPS receiver clock bias in positioning, and indicates that the base receiver clock bias is in the high frequency components of $\alpha_1^i(t)$. Due to the mixture of low frequency and high frequency components, it is not straightforward to predict $\alpha_1^i(t)$.
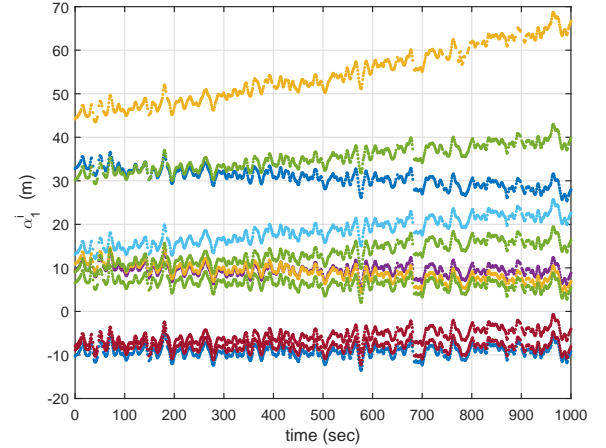

Fig. 6. All corrections $\{\alpha_1^i(t)\}$ for L1 code measurements over a 1000s interval. Different colors are for different satellites.
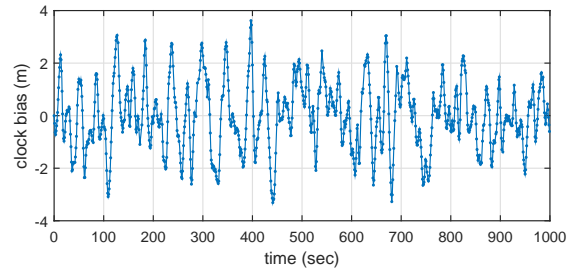

Fig. 7. GPS clock bias (fine-steering enabled) estimates from single epoch positioning.

Define

$$\beta_1^i(t) \triangleq \alpha_1^i(t) - c\delta t_b(t)$$
$$= E_{cm1}^{ib}(t) + n_{\rho_1}^{ib}(t), \tag{64}$$

$$\beta_2^i(t) \triangleq \alpha_2^i(t) - c\delta t_b(t)$$
$$= E_{cm2}^{ib}(t) + n_{\rho_2}^{ib}(t), \tag{65}$$

$$\beta_3^i(t) \triangleq \alpha_3^i(t) - c\delta t_b(t)$$
$$= E_{cm3}^{ib}(t) + \lambda N_1^{ib}(t) + n_{\varphi_1}^{ib}(t), \tag{66}$$

$$\beta_4^i(t) \triangleq \alpha_4^i(t) - c\delta t_b(t)$$
$$= E_{cm4}^{ib}(t) + \lambda N_2^{ib}(t) + n_{\varphi_2}^{ib}(t), \tag{67}$$

7

then another version of single-differenced measurements can be defined as

$$^{\beta}\tilde{\rho}_{r_1}^{id} = \tilde{\rho}_{r_1}^i - \beta_1^i, \tag{68}$$

$$^{\beta}\tilde{\rho}_{r_2}^{id} = \tilde{\rho}_{r_2}^i - \beta_2^i, \tag{69}$$

$$\lambda_1 {}^{\beta}\tilde{\varphi}_{r1}^{id} = \lambda_1 \tilde{\varphi}_{r1}^i - \beta_3^i, \tag{70}$$

$$\lambda_2 {}^{\beta}\tilde{\varphi}_{r2}^{id} = \lambda_1 \tilde{\varphi}_{r2}^i - \beta_4^i, \tag{71}$$

with the models

$$^{\beta}\tilde{\rho}_{r_1}^{id}(t) = \|\mathbf{p}_r(t) - \hat{\mathbf{p}}^i(t)\|_2 + c\delta t_r(t) \\ + M_{\rho_1}^i(t) + n_{\rho_1}^{id}(t), \tag{72}$$

$$^{\beta}\tilde{\rho}_{r_2}^{id}(t) = \|\mathbf{p}_r(t) - \hat{\mathbf{p}}^i(t)\|_2 + c\delta t_r(t) \\ + M_{\rho_2}^i(t) + n_{\rho_2}^{id}(t), \tag{73}$$

$$\lambda_1 {}^{\beta}\tilde{\varphi}_{r1}^{id}(t) = \|\mathbf{p}_r(t) - \hat{\mathbf{p}}^i(t)\|_2 + c\delta t_r(t) \\ + \lambda_1 N_1^{id}(t) + M_{\varphi_1}^i(t) + n_{\varphi_1}^{id}(t), \tag{74}$$

$$\lambda_1 {}^{\beta}\tilde{\varphi}_{r2}^{id}(t) = \|\mathbf{p}_r(t) - \hat{\mathbf{p}}^i(t)\|_2 + c\delta t_r(t) \\ + \lambda_2 N_2^{id}(t) + M_{\varphi_2}^i(t) + n_{\varphi_2}^{id}(t). \tag{75}$$

Note that the only difference between eqns. (40)-(43) and eqns. (72)-(75), are eqns. (72)-(75) the rover receiver biases $c\delta t_r(t)$ are not mixed with the base receiver biases $c\delta t_b(t)$. It can be proved that the positioning results from these two versions of single-differenced measurements are identical. If the base receiver locks are maintained, then $\lambda N_1^{ib}(t) \equiv \lambda N_1^{ib} \in \mathbb{Z}$ and $\lambda N_2^{ib}(t) \equiv \lambda N_2^{ib} \in \mathbb{Z}$ are integral constants. Also, the common errors $\{E_{cmj}^{ib}(t)\}_{j=1}^4$ are slowly-varying variables, thus a linear regression based method is proposed, to estimate the corrections $\{\beta_j^i(t)\}_{j=1}^4$ in real-time. Thus, the single-differenced measurements $^{\beta}\tilde{\rho}_{r_1}^{id}$, $^{\beta}\tilde{\rho}_{r_2}^{id}$, $^{\beta}\tilde{\varphi}_{r2}^{id}$, $^{\beta}\tilde{\varphi}_{r2}^{id}$ can be calculated. The procedures of the proposed method are as follows

- Pass $\{\alpha_1^i(t_{1-d}), \ldots, \alpha_1^i(t_{K-d})\}$, computed through eqn. (24) for each satellite, to a low-pass filter (e.g. moving average filter) $C(s)$, to obtain the output $\{\hat{\alpha}_1^i(t_{1-d}), \ldots, \hat{\alpha}_1^i(t_{K-d})\}$,
- Take the median of the error $\epsilon_1^i(t) \triangleq \alpha_1^i(t) - \hat{\alpha}_1^i(t)$, over all available satellites ($i = 1, \ldots, m$), to get an estimate of the base clock bias

$$clk(t) \triangleq median(\epsilon_1^i(t)). \tag{76}$$

Fig. 8 shows an example for this step.
- Evaluate $\{\gamma_j^i(t)\}_{j=1}^4$ as

$$\gamma_j^i(t) \triangleq \alpha_j^i(t) - clk(t),$$

and keep them in circular buffers with length L. Use $\{\gamma_j^i(t_{K-d-L+1}), \ldots, \gamma_j^i(t_{K-d})\}$ to fit a linear model $\hat{\beta}_j^i(t)$, for estimating $\beta_j^i(t_K)$.
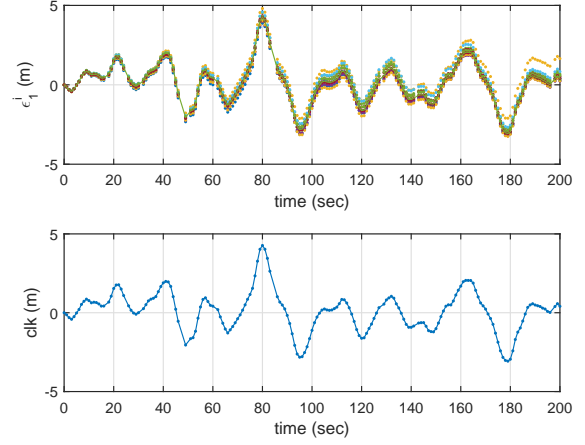- Finally, the rover uses the estimated DGPS measure-

Fig. 8. Filtered noise $\epsilon_1^i(t)$ and the estimate of the base clock bias $clk(t)$.

ments

$$^{\gamma}\tilde{\rho}_{r_1}^{id} = \tilde{\rho}_{r_1}^i - \hat{\beta}_1^i, \tag{77}$$

$$^{\gamma}\tilde{\rho}_{r_2}^{id} = \tilde{\rho}_{r_2}^i - \hat{\beta}_2^i, \tag{78}$$

$$\lambda_1 {}^{\gamma}\tilde{\varphi}_{r1}^{id} = \lambda_1 \tilde{\varphi}_{r1}^i - \hat{\beta}_3^i, \tag{79}$$

$$\lambda_2 {}^{\gamma}\tilde{\varphi}_{r2}^{id} = \lambda_1 \tilde{\varphi}_{r2}^i - \hat{\beta}_4^i, \tag{80}$$

with the models

$$^{\gamma}\tilde{\rho}_{r_1}^{id}(t) = \|\mathbf{p}_r(t) - \hat{\mathbf{p}}^i(t)\|_2 + c\delta t_r(t) \\ + M_{\rho_1}^i(t) + n_{\rho_1}^{id}(t), \tag{81}$$

$$^{\gamma}\tilde{\rho}_{r_2}^{id}(t) = \|\mathbf{p}_r(t) - \hat{\mathbf{p}}^i(t)\|_2 + c\delta t_r(t) \\ + M_{\rho_2}^i(t) + n_{\rho_2}^{id}(t), \tag{82}$$

$$\lambda_1 {}^{\gamma}\tilde{\varphi}_{r1}^{id}(t) = \|\mathbf{p}_r(t) - \hat{\mathbf{p}}^i(t)\|_2 + c\delta t_r(t) \\ + \lambda_1 N_1^{id} + M_{\varphi_1}^i(t) + n_{\varphi_1}^{id}(t), \tag{83}$$

$$\lambda_1 {}^{\gamma}\tilde{\varphi}_{r2}^{id}(t) = \|\mathbf{p}_r(t) - \hat{\mathbf{p}}^i(t)\|_2 + c\delta t_r(t) \\ + \lambda_2 N_2^{id} + M_{\varphi_2}^i(t) + n_{\varphi_2}^{id}(t), \tag{84}$$

to do positioning.

Note that in eqns. (83)-(84), integer ambiguities N_1^{id} and N_2^{id} remove the time stamp, since it is assumed that the phase-lock-loop of the base receiver for the i-th satellite is maintained. This assumption is often satisfied since most of base stations are established in a good electromagnetic environment, e.g. on the top of the mountain or high buildings with high quality antenna (see CORS stations [3]). For low-cost single-frequency receiver base stations in noisy environment, the proposed correction calculation method can significantly enhance the robustness of the differential positioning. The reason is that all data in a window is used for the correction fitting which improves the degree-of-freedom of the estimation problem. To handle faulty measurements caused by unexpected noise or undetected cycle slips, a robust optimization technique can be applied to the proposed correction calculation method.

Fig. 9 shows the overall process of the differential correction calculation for L1 code measurements. Comparing

$\gamma_1^i(t)$ with $\alpha_1^i(t)$, it can be seen that the high frequency component caused by the clock bias and the measurement noise are removed, such that a linear model can be fit to calculate $\hat{\beta}_1^i(t)$.
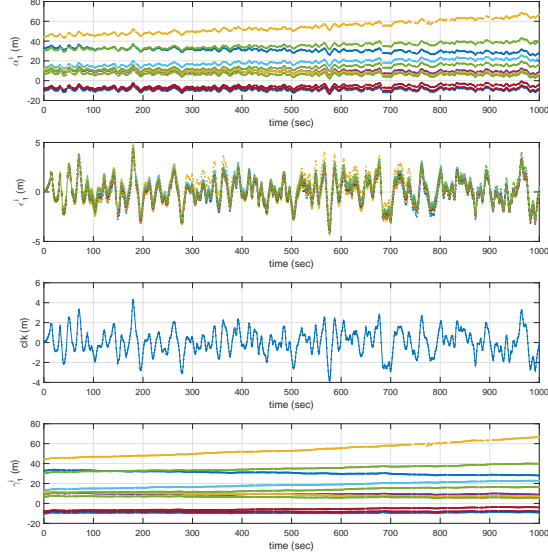

Fig. 9.   Real-time correction computation process.

Several experimental results of differential GPS are presented to illustrate the proposed method. Since position performance is of interest, in all the following experiments, the rover is stationary over a 30-minute window. The ground truth of rover's global position is surveyed with geodetic grade dual frequency receiver and antenna. The survey data was processed by Online Positioning User Service (OPUS) [14] aided with measurements from nearby differential stations. The accuracy of the survey is $\pm(0.02, 0.02, 0.02)\ m$ in North-East-Down directions.

Six experiments were performed: no-baseline, short-baseline and long-baseline. The results are tabulated in Table IV. Herein, the baseline is defined as the distance between the rover receiver and the base station receiver. Among the experiments, no-baseline and short-baseline experiment data was collected with UC Riverside NTRIP station (ntrip.engr.ucr.edu@2101) and a rover receiver and antenna on UCR campus. In particular, no-baseline experiments were done by connecting the base and rover receivers to the same antenna. The long-baseline experiment data was collected with ESRI GISA NTRIP station (esricaster.esri.com@2101) and a rover receiver and antenna on UCR campus. Fig. 10 and 11 show that even in the no-baseline condition, there exists a time delay in the NTRIP stream. The base correction computed by the proposed method can cancel the common error and realize unbiased positioning result. Fig. 12 and 13 show the expected centimeter-level accuracy of the RTK technique. Fig. 14 to 21 show that although the positioning error of DGPS grows as the baseline expands,
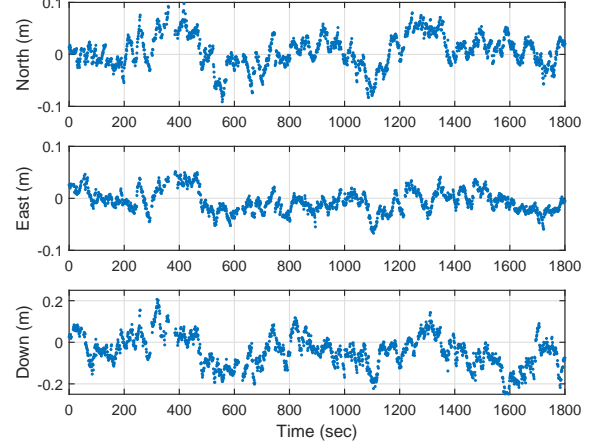

Fig. 10.   L1 DGPS Code-only positioning: no-baseline result.

the RTK technique with the calculated base corrections still can realize centimeter level positioning accuracy.

TABLE II

BASE CORRECTION COMPUTATION EXPERIMENTS

Baseline (km)	Measurement used	Ntrip delay (sec)	Figure number
0	L1 Code	3-5	10, 11
0	L1 Code+Phase	3-5	12, 13
< 1	L1 Code	3-5	14, 15
< 1	L1 Code+Phase	3-5	16, 17
15	L1 Code	1-2	18, 19
15	L1 Code+Phase	1-2	20, 21

V. POSITION ESTIMATION

A. Least Squares Position using Pseudorange

B. DGPS Relative Position using Carrier Phase

  1) Selection of Observations:
  2) Baseline Solution using Double Differences:
  3) Stochastic Model:

VI. MODEL ESTIMATION

A. Troposphere Model

The troposphere is the lower part of the atmosphere extending nominally to 50 km above the surface of the planet. The troposphere is composed essentially of electrically neutral particles and for L-Band signals it is non-dispersive. The troposphere experiences changes in temperature, pressure, and humidity associated with weather. Because these same variables affect the density of the air mass along the signal path and the index-of-refraction is a function of air mass density, tropospheric conditions affect the measured time-of-propagation with the measured value being larger than that the geometric range.

Tropospheric delays

$$T_r^s = \frac{1}{c} \int_{\gamma_T} (\eta(l) - 1) dl \qquad (85)$$

can be quite considerable ($\sim 30m$) for satellites at low elevations. Tropospheric delay errors are consistent between
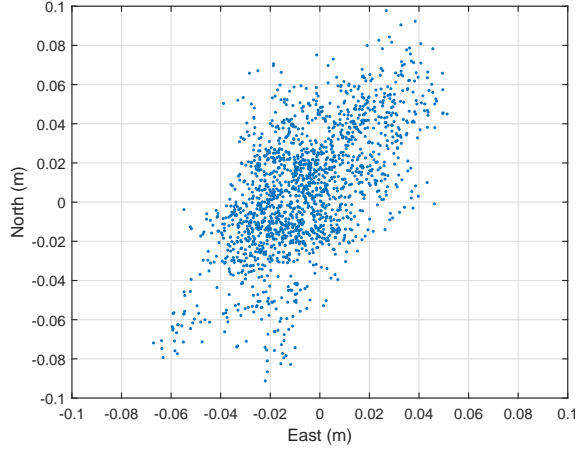
Fig. 11. L1 DGPS Code-only positioning: no-baseline result on the tangent plane.
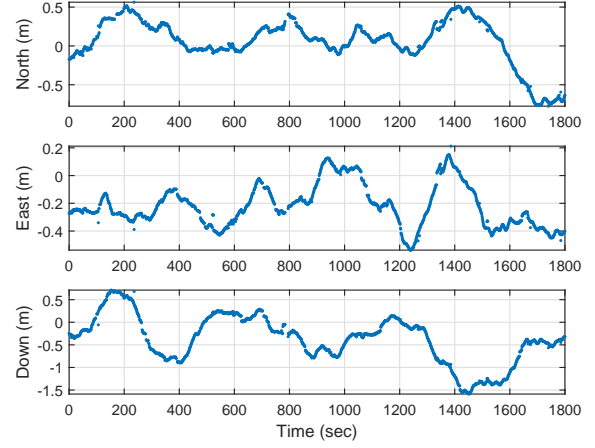

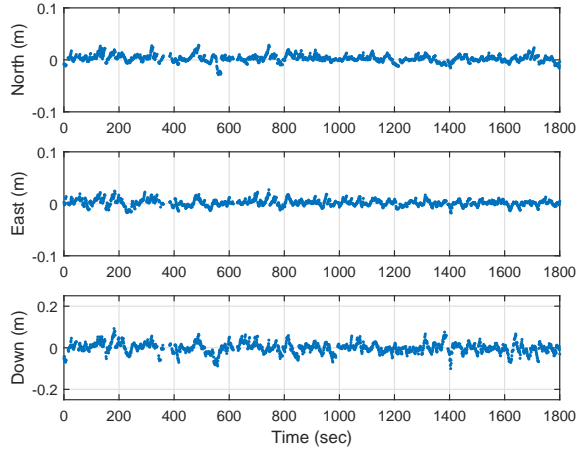Fig. 14. L1 DGPS Code-only positioning: short-baseline result.

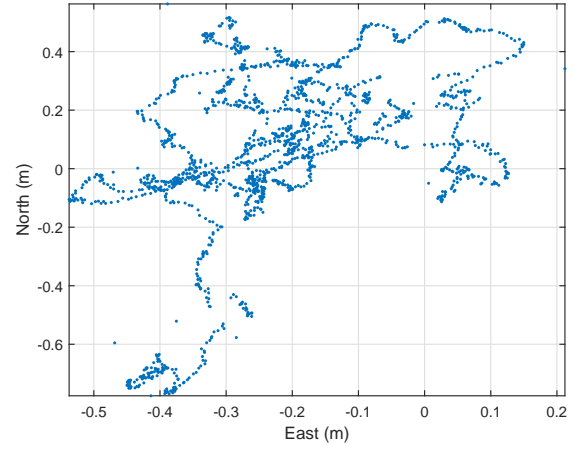Fig. 12. L1 DGPS Code+Phase positioning: no-baseline result.

Fig. 15. L1 DGPS Code-only positioning: short-baseline result on the tangent plane.
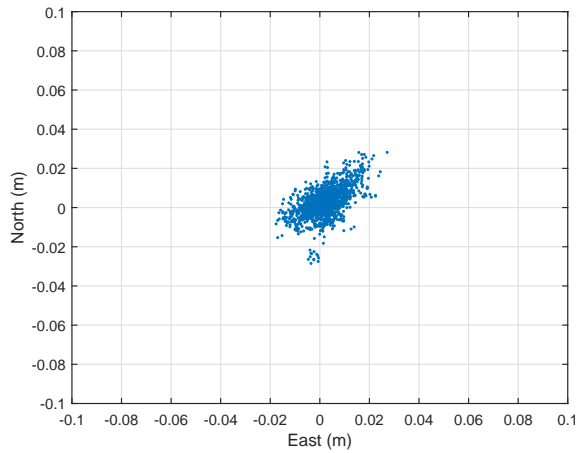

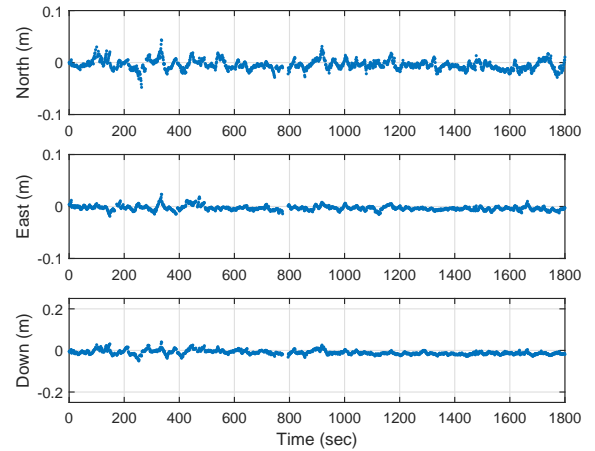Fig. 13. L1 DGPS Code+Phase positioning: no-baseline result on the tangent plane.

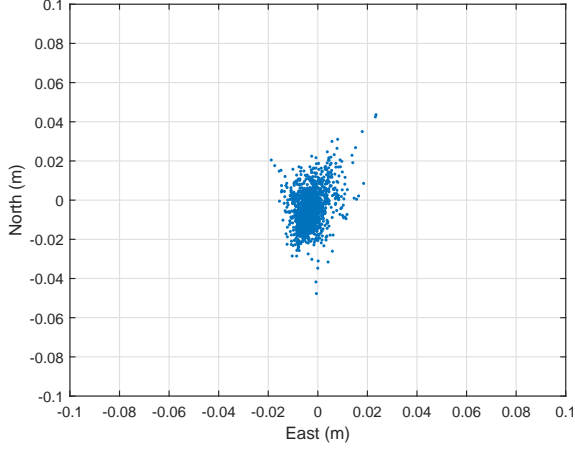Fig. 16. L1 DGPS Code+Phase positioning: short-baseline result.

10

Fig. 17. L1 DGPS Code+Phase positioning: short-baseline result on the tangent plane.
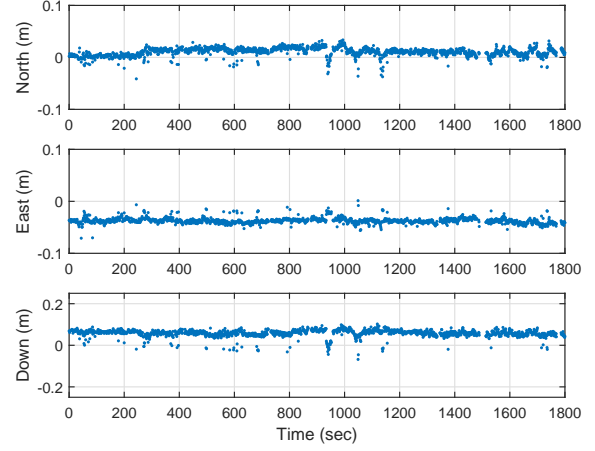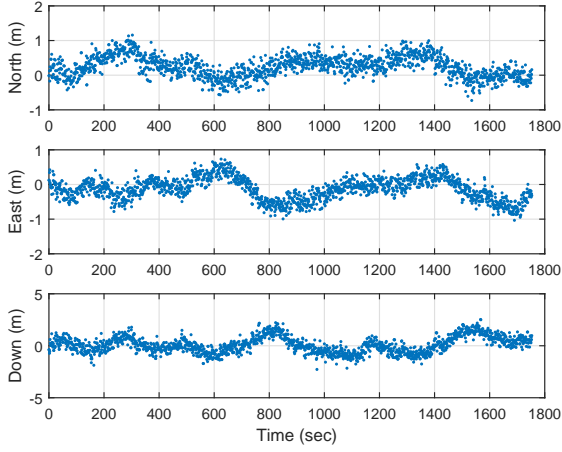

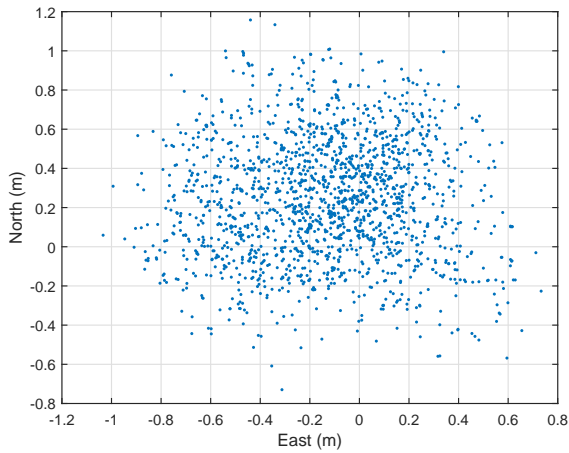Fig. 18. L1 DGPS Code-only positioning: long-baseline result.

Fig. 19. L1 DGPS Code-only positioning: long-baseline result on the tangent plane.

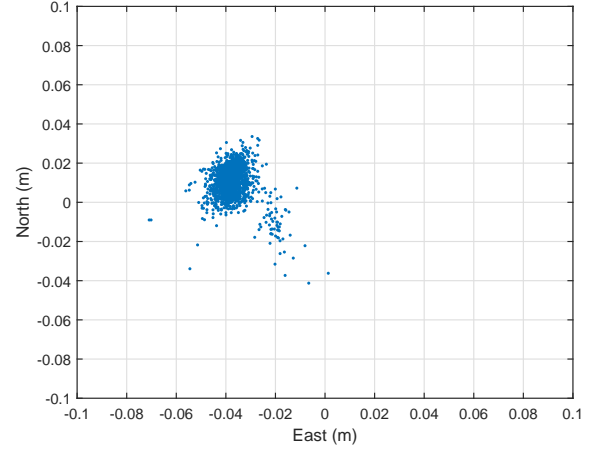Fig. 20. L1 DGPS Code+Phase positioning: long-baseline result.

Fig. 21. L1 DGPS Code+Phase positioning: long-baseline result on the tangent plane.

the L1 and L2 signals and carrier and code signals. The tropospheric delay cannot be computed from the GPS observables; therefore, tropospheric effects are compensated via models. For most users, especially in navigation application, the input parameters for the models are average or typical values for the user location. Users with higher accuracy requirements can add meteorological instruments to sense the model input variables or may use differential GPS methods.

The refractive index is affected differently by the water vapor and by the dry components (e.g., nitrogen and oxygen) of the troposphere, so tropospheric models account for these wet and dry pressures separately. The wet component is difficult to predict due to local variations in the water vapor content of the troposphere and accounts for approximately 10% of the tropospheric delay. The dry component is relatively easier to predict and accounts for approximately 90% of the tropospheric delay.

Several models exist for the tropospheric wet and dry components [15]–[18]. The models contain two parts. The first part of the model is the estimate of the zenith delay.

11

The second part is a slant factor to account for the satellite elevation. For example, the Chao model is

$$\delta\rho_{dry} = 2.276 \times 10^{-5} P \tag{86}$$

$$F_{dry} = \frac{1}{\sin(E) + \frac{0.00143}{\tan(E) + 0.0445}} \tag{87}$$

$$\delta\rho_{wet} = 4.70 \times 10^2 \frac{e_o^{1.23}}{T^2} + 1.705 \times 10^6 \alpha \frac{e_o^{1.46}}{T^3} \tag{88}$$

$$F_{wet} = \frac{1}{\sin(E) + \frac{0.00035}{\tan(E) + 0.017}} \tag{89}$$

$$\delta\hat{\rho}_T = \delta\rho_{dry} F_{dry} + \delta\rho_{wet} F_{wet} \tag{90}$$

where δp is the tropospheric delay expressed in meters, P is the atmospheric pressure in $\frac{N}{m^2}$, T is the temperature in $^\circ K$, e_o is the partial pressure of water vapor in millibars, α is the temperature lapse rate in $^\circ K$ per meter, and E is the satellite elevation angle. The partial pressure e_o can be computed from T and the relative humidity. In most navigation applications, tropospheric delay is not compensated by equations such as this due to the expense involved in measuring the required formula input variables. Instead, simplified formulas have been determined which only depend on satellite elevation, receiver altitude, and satellite altitude.

The Magnavox, Collins, Remondi algorithms are, respectively,

$$\delta\hat{\rho}_{T_M} = \frac{2.208}{\sin(E)} \left(e^{\frac{-h_r}{6900}} - e^{\frac{-h_s}{6900}} \right) \tag{91}$$

$$\delta\hat{\rho}_{T_C} = \frac{2.4225}{0.026 \sin(E)} e^{\frac{-h_r}{7492.8}} \tag{92}$$

$$\delta\hat{\rho}_{T_R} = \frac{2.47}{\sin(E) + 0.0121} e^{-133 h_r} \tag{93}$$

where h_r and h_s are the receiver and satellite altitudes in meters and the rest of the variables are as previously defined. The Magnavox and Collins tropospheric correction models match each other and the Chao model (for standard assumptions) to within one meter for elevation angles greater than 15 degrees. The Magnavox model matches the Chao model more closely for elevation angles less than 5 degrees [17].

B. Ionosphere Model

The ionosphere is the layer of the atmosphere with altitude between 50 and 1000 km that contains free electrons and positively charged molecules. The level of ionization is affected by solar activity, season, and time-of-day. Changes in the level of ionization affect the refractive index along the path through the ionosphere and therefore affect the travel time measured by the receiver.

For L-Band (e.g., GPS) signals, the ionosphere is a dispersive medium. For a modulated signal traveling through dispersive medium, the medium will affect the carrier and modulating signals differently. Let

$$y(t) = m(t) \sin(\omega_c t) \tag{94}$$

where $m(t)$ represents a modulating signal with bandwidth significantly smaller than the carrier frequency $\omega_c = 2\pi f_c$.

The modulating signal $m(t)$ propagates at the *group velocity* as determined by the group refractive index $\eta_g(l)$ while the carrier signal $\sin(\omega_c t)$ propagates at the *phase velocity* determined by the phase refractive index $\eta_\phi(l)$. Detailed analyses are presented on p. 136 in [19] and p. 309 in [8]. To first order, the phase and group refractive indices can be modeled, respectively, as

$$\eta_\phi(l) = 1 - \frac{\kappa}{f_c^2} N_e(l) \tag{95}$$

$$\eta_g(l) = \eta_\phi(l) + f_c \frac{d\eta_\phi}{df_c} \tag{96}$$

$$= 1 + \frac{\kappa}{f_c^2} N_e(l) \tag{97}$$

where $\kappa = 40.28$ and $N_e(l)$ is the density of free electrons at location $\gamma(l)$. Therefore, using the first term in eqn. (8.58), the delay experienced by the code is

$$\delta t_g = \frac{1}{c} \frac{\kappa}{f_c^2} \int_{\gamma I} N_e(l) dl \tag{98}$$

and the delay experience by the carrier phase is

$$\delta t_\phi = -\frac{1}{c} \frac{\kappa}{f_c^2} \int_{\gamma I} N_e(l) dl. \tag{99}$$

To first order, the group and phase experience the same delay with the same magnitude, but opposite in sign. The code is delayed while the phase is advanced. This phenomenon is referred to as *code carrier divergence*.

Defining the total electron count (TEC) along the path as

$$TEC = \int_{\gamma I} N(l) dl \tag{100}$$

and defining $I_r^i = \frac{40.28}{f_1 f_2} TEC$, then at the L1 frequency the code and phase delays can be expressed simply as

$$\delta t_g = \frac{1}{c} \frac{f_2}{f_1} I_r^i, \tag{101}$$

$$\delta t_\phi = -\frac{1}{c} \frac{f_2}{f_1} I_r^i. \tag{102}$$

At the L2 frequency the code and phase delays are similarly expressed as

$$\delta t_g = \frac{1}{c} \frac{f_1}{f_2} I_r^i, \tag{103}$$

$$\delta t_\phi = -\frac{1}{c} \frac{f_1}{f_2} I_r^i. \tag{104}$$

Two frequency receivers are designed to take advantage of the frequency dependence to estimate I_r^i as is described in Section 8.6.

Single frequency receivers must rely on either differential operation or an ionospheric delay model. One such approach based on parameters broadcast by the satellite is described in Section C.5 of Appendix C in [10]. This Klobuchar model is expected to compensate for approximately 50% of the ionospheric delay [1]. Since TEC is path dependent, the ability of differential GPS techniques to compensate for ionospheric errors will depend on the user to reference station baseline vector.

C. Ionospheric error correction

The following equations are used in the calculation for Ionospheric error correction: The receiver latitude is

$$\psi = \frac{0.0137}{E + 0.11} - 0.022, \tag{105}$$

$$\phi_I = \phi_u + \psi \cos Az. \tag{106}$$

If $\phi_I > 0.416$, set $\phi_I = 0.416$, otherwise if $\phi_I < -0.416$, set $\phi_I = -0.416$. The receiver longitude is

$$\lambda_I = \lambda_u + \frac{\psi \sin Az}{\cos \phi_I} \tag{107}$$

where E is the elevation angle in semi circles, Az is the azimuth angle in semi circles, ϕ_u is receiver latitude in semi circles, λ_u is the receiver longitude in semi circles.

$$\phi_m = \phi_I + 0.064 \cos(\lambda_I - 1.617) \tag{108}$$

$$AMP = \left\{ \begin{array}{ll} \sum_{i=0}^{3} \alpha_i \phi_m^i, & \text{if } AMP > 0 \\ 0, & \text{if } AMP < 0 \end{array} \right\} \tag{109}$$

$$PER = \left\{ \begin{array}{ll} \sum_{i=0}^{3} \beta_i \phi_m^i, & \text{if } PER \geq 72000 \\ 0, & \text{if } PER < 72000 \end{array} \right\} \tag{110}$$

$$F = 1 + 16(0.53 - E)^3 \tag{111}$$

$$t = 43200\lambda_I + TOW \tag{112}$$

$$limit_t = \left\{ \begin{array}{ll} t = t - 86400, & \text{if } t > 86400 \\ t = t + 86400, & \text{if } t < 0 \end{array} \right\} \tag{113}$$

$$x = \frac{2\pi(t - 50400)}{PER} \tag{114}$$

$$T_{iono} = \left\{ \begin{array}{ll} F(5 \times 10^{-9} + AMP(1 - \frac{x^2}{2} + \frac{x^4}{24})), & \text{if } |x| < 1.57 \\ F \cdot 5 \times 10^{-9}, & \text{if } |x| > 1.57 \end{array} \right. \tag{115}$$

$$\delta_{iono} = cT_{iono} \tag{116}$$

D. Range from receiver to satellite calculation

The ECEF position of the receiver, r_r, is calculated using the state estimate, $\hat{x}_p$ at 1pps,

Satellite position is calculated based on the satellite ephemeris at time t. The Remondi algorithm is used for satellite velocity calculation. The time t is equal to current GPS time subtracted propagation time. An iterative algorithm is used to determine the propagation delay from satellite to the receiver.

First: set $i = 0$, and $t_p(i) = 0.0065$, then iterate the following steps:

1) $t_{Tx} = t_{gps} - t_p(i)$
2) Calculate Satellite ECEF position and satellite velocity
3) Calculate earth rotation angle during this propagation delay period
4) Compensate satellite position with this rotation angle
5) Calculate the range from receiver to this satellite and update the propagation delay
6) increment i by 1, go back to step 1 with maximum of 5 iterations.

Now calculate elevation angle E and azimuth angle Az for the ionospheric error correction calculation. Transform range vector in ECEF to navigation frame, N, first

$$r = R_E^N(r_{sat} - r_{user}) \tag{117}$$

$$Az = \tan^{-1} \frac{r(2)}{r(1)} \tag{118}$$

$$El = \tan^{-1} \frac{-r(3)}{\sqrt{r(1)^2 + r(2)^2}} \tag{119}$$

E. Satellite position calculation

TABLE III

Ephemeris parameters	
M_0	Mean anomaly at reference time.
Δ_n	Mean motion difference from computed value.
e	Eccentricity of the orbit.
$\sqrt{A}$	Square root of the semi major axis.
Ω_0	Longitude of ascending node of orbit plane at reference time.
i_0	Inclination angle at reference time.
ω	Argument of perigee.
$\dot{\Omega}$	Rate of right ascension.
$\dot{i}$	Rate of Inclination angle.
C_{uc}	Amplitude of the cosine harmonic correction to the argument of latitude.
C_{us}	Amplitude of the sine harmonic correction to the argument of latitude.
C_{rc}	Amplitude of the cosine harmonic correction to the orbit radius.
C_{rs}	Amplitude of the sine harmonic correction to the orbit radius.
C_{ic}	Amplitude of the cosine harmonic correction to the angle of inclination.
C_{ic}	Amplitude of the sine harmonic correction to the angle of inclination.
t_{oe}	Reference time for ephemeris.
$IODE$	Issue of Data (Ephemeris).

TABLE IV

Constant Values	
$\mu = 3.986005 \times 10^{14} \frac{m^3}{s^2}$	WGS-84: Earths gravitational parameter.
$\dot{\Omega}_e = 7.2921151467^{-5} \frac{rad}{s}$	WGS-84: Earths rotation rate.
$\pi = 3.1415926535898$	GPS standard value for π.
$n_0 = \sqrt{\mu/A^3} \frac{rad}{s}$	Computed mean motion.
$n = n_0 + \Delta n$	Corrected mean motion.
$t_k = t - t_{oe}$	Time from ephemeris reference time.
$M_k = M_0 + nt_k$	Mean Anomaly.
$M_k = E_k - e \sin(E_k)$	Keplers equation for eccentric anomaly E_k.

Algorithm 1 Eccentric anomaly

1: Set $E_k = M_k$, $i = 0$
2: **while** $((\delta E_k > 1 \times 10^{-10})$ & $(i < 10))$
3: $\quad i = i + 1$
4: $\quad \delta E_k = \frac{-((E_k - e \sin(E_k)) - M_k)}{1 - e \cos(E_k)}$
5: $\quad E_k = E_k + \delta E_k$

True anomaly

$$v_k = \tan^{-1} \frac{\sin v_k}{\cos v_k} \tag{120}$$

$$= \tan^{-1} \frac{\sqrt{1 - e^2} \sin E_k/(1 - e \cos E_k)}{(\cos E_k - e)/(1 - e \cos E_k)} \tag{121}$$

Argument of latitude

$$\phi_k = v_k + \omega \tag{122}$$

Argument of latitude correction 2nd harmonic perturbations

$$\delta u_k = C_{us} \sin 2\phi_k + C_{uc} \cos 2\phi_k \tag{123}$$

Radius correction 2nd harmonic perturbations

$$\delta r_k = C_{rs} \sin 2\phi_k + C_{rc} \cos 2\phi_k \tag{124}$$

Inclination correction 2nd harmonic perturbations

$$\delta i_k = C_{is} \sin 2\phi_k + C_{ic} \cos 2\phi_k \tag{125}$$

Corrected argument of latitude

$$u_k = phi_k + \delta u_k \tag{126}$$

Corrected radius

$$r_k = A(1 - e \cos E_k) + \delta r_k \tag{127}$$

Corrected inclination

$$i_k = i_0 + \delta i_k + \dot{i} t_k \tag{128}$$

Satellite position in orbit plane

$$x'_k = r_k \cos u_k \tag{129}$$
$$y'_k = r_k \sin u_k \tag{130}$$

Corrected longitude of ascending node

$$\Omega_k = \Omega_0 + (\dot{\Omega} - \dot{\Omega}_e)t_k - \dot{\Omega}_e t_{oe} \tag{131}$$

Satellite position in ECEF coordinates

$$x_k = x'_k \cos \Omega_k - y'_k \cos i_k \sin \Omega_k \tag{132}$$
$$y_k = x'_k \sin \Omega_k - y'_k \cos i_k \cos \Omega_k \tag{133}$$
$$z_k = y'_k \sin i_k \tag{134}$$

Rate of change of eccentric anomaly

$$\dot{E}_k = \frac{n}{1 - e \cos E_k} \tag{135}$$

Rate of change of true anomaly

$$\dot{t}_{ak} = \frac{\sin E_k \dot{E}_k (1 + e \cos v_k)}{\sin v_k (1 - e \cos E_k)} \tag{136}$$

Rate of change of argument of latitude

$$\dot{u}_k = \dot{t}_{ak} + 2 \left(C_{us} \cos(2u_k) - C_{uc} \sin(2u_k) \right) \dot{t}_{ak} \tag{137}$$

Rate of change of radius

$$\dot{r}_k = \frac{a \cdot e \cdot n \sin E_k}{1 - e \cos E_k} + 2 \left(C_{rs} \cos(2u_k) - C_{rc} \sin(2u_k) \right) \dot{t}_{ak} \tag{138}$$

Rate of change of inclination

$$\dot{i}_k = i + 2 \left(C_{is} \cos(2u_k) - C_{ic} \sin(2u_k) \right) \dot{t}_{ak} \tag{139}$$

Rate of change of longitude of ascending node

$$\dot{\Omega}_k = \dot{\Omega} - \dot{\Omega}_e \tag{140}$$

$$\dot{x}_{pk} = \dot{r}_k \cos u_k - y'_k \dot{u}_k \tag{141}$$
$$\dot{y}_{pk} = \dot{r}_k \sin u_k - x'_k \dot{u}_k \tag{142}$$

Satellite velocity in ECEF coordinates

$$V_x = (\dot{x}_{pk} - y'_k \cos(i_k)\dot{\Omega}_k) \cos \Omega_k \tag{143}$$
$$- (x'_k \dot{\Omega}_k + \dot{y}_{pk} \cos(i_k) - y'_k \sin(i_k)\dot{i}_k) \sin \Omega_k \tag{144}$$
$$V_y = (\dot{x}_{pk} - y'_k \cos(i_k)\dot{\Omega}_k) \sin \Omega_k \tag{145}$$
$$- (x'_k \dot{\Omega}_k + \dot{y}_{pk} \cos(i_k) - y'_k \sin(i_k)\dot{i}_k) \cos \Omega_k \tag{146}$$
$$V_z = \dot{y}_{pk} \sin(i_k) + y'_k \cos(i_k)\dot{i}_k \tag{147}$$

F. Satellite clock error correction

The satellite clock error correction, δ_c^s, is computed by the following equations

$$\delta t_R = F \cdot e\sqrt{A} \sin E_k \tag{148}$$
$$F = -4.442807633 \times 10^{-10} \tag{149}$$
$$\delta_c^s = c(\alpha_{f0} + \alpha_{f1}(t - t_{oc}) + \alpha_{f2}(t - t_{oc})^2 + \delta t_R) \tag{150}$$

where δt_R is in units of seconds, F is in $sec/\sqrt{m}$, and δ_c^s is in meters.

REFERENCES

[1] Anonymous, "Global Positioning System Interface Specification," U.S. Air Force Global Positioning Systems Directorate Systems Engineering and Integration, Report IS-GPS-200-H, 21 March 2014.

[2] ——, "Global Positioning Wide Area Augmentation System (WAAS) Performance Standard," Federal Aviation Administration, Report, 31 October 2008.

[3] R. A. Snay and M. Tomás Soler, "Continuously operating reference station (CORS): History, applications, and future enhancements," *Journal of Surveying Engineering*, vol. 134, no. 4, 2008.

[4] P. Gary and C. E. Fly, "NDGPS assessement final report," U.S. Department of Transportation, Tech. Rep., 2008.

[5] D. Dettmering and G. Weber, "The euref-ip ntripbroadcaster: Real-time gnss data for europe," in *Proceedings of the IGS Workshop*, Astronimical Institute University of Bern, Switzerland, 2004, pp. 1–8.

[6] RTCM Special Committee No. 104, "RTCM Standard 10403.1, Differential GNSS Services, Version 3," Radio Technical Commission for Maritime Services, Tech. Rep., 2011.

[7] P. Gary and C. E. Fly, "RTCM Standard 10410.1, Networked Transport of RTCM via Internet Protocol (Ntrip), Version 2.0," Radio Technical Commission for Maritime Services, Tech. Rep., 2011.

[8] E. Kaplan and C. Hegarty, *Understanding GPS Principles and Applications, 2nd Ed.* Artch House, 2006.

[9] Anonymous, "Global positioning system standard positioning service performance standard," U.S. Department of Defense, Tech. Rep., 2008.

[10] J. A. Farrell, *Aided Navigation: GPS with High Rate Sensors*. McGraw Hill, 2008.

[11] X. W. Chang and T. Zhou, "MILES: MATLAB package for solving Mixed Integer LEast Squares problems," *Journal of Geodesy*, 2007.

[12] P. J. G. Teunissen, "The least-squares ambiguity decorrelation adjustment: a method for fast GPS integer ambiguity estimation," *Journal of Geodesy*, 1994.

[13] X. W. Chang and T. Zhou, "MLAMBDA: a modified LAMBDA method for integer least-squares estimation," *Journal of Geodesy*, 2005.

[14] "Online Positioning User Service: http://www.ngs.noaa.gov/opus/."

[15] Anonymous, "Phase I NAVSTAR/GPS major field test objective report thermostatic correction," Navstar/GPS Joint Program Office, Space and Missile Systems Organization, Los Angeles Air Force Station, Los Angeles, California, Tech. Rep., 4 May 1979.

[16] A. E. Niell, "Global mapping functions for the atmosphere delay at radio wavelengths," *Journal of Geophysical Research*, vol. 101(B2), pp. 3227–3246, 1996.

[17] J. Shockley, "Consideration of troposheric model corrections for differential gps," SRI International, Tech. Rep., February 1984.

[18] J. J. Spilker, *Tropospheric effects on GPS*. AIAA - Global Positioning System: Theory and Applications, 1996, vol. 1.

[19] P. Misra and P. Enge, *Global Positioning System: Signals, Measurements, and Performance*. Ganga-Jamuna Press, 2001.